Determination of the pore size distribution around an injected borehole using non-Newtonian fluids

Martin Lanzendörfer, Jiří Mls
joint work with J. Najser, J. Roháč, S. Safari, M. Slavík, T. Weiss

Charles University, Faculty of Science, IHEGAG
Prague

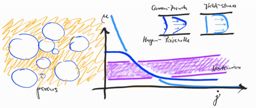

Supported by Czech Science Foundation project GA21-27291S (years 2021-2023).

I. (Non-Newtonian) shear-thinning fluids

Shear-thinning fluids.
Power-law model.
Hagen–Poiseuille flow.
In hydrogeology.

Non-Newtonian fluids

Newtonian (incompressible) fluid

such as water, is characterized by the consitutive relations

$$\mathbf{T} = -p\mathbf{I} + 2\mu\,\mathbf{D}, \qquad \operatorname{tr}\mathbf{D} = \operatorname{div}\mathbf{v} = 0,$$

μ dynamic viscosity, $\mu > 0$

p, $\mathbf{v}$ pressure, velocity

$\mathbf{T}$, $\mathbf{I}$, $\mathbf{D}$ Cauchy stress tensor, Identity tensor, symmetric part of the velocity gradient

Non-Newtonian fluids

Newtonian (incompressible) fluid

such as water, is characterized by the consitutive relations

$$\mathbf{T} = -p\mathbf{I} + 2\mu\,\mathbf{D}, \qquad \operatorname{tr}\mathbf{D} = \operatorname{div}\mathbf{v} = 0,$$

μ dynamic viscosity, $\mu > 0$

p, $\mathbf{v}$ pressure, velocity

$\mathbf{T}$, $\mathbf{I}$, $\mathbf{D}$ Cauchy stress tensor, Identity tensor, symmetric part of the velocity gradient

Non-Newtonian fluids

are *all others*, and they are many. . .

- die swelling (Barus effect), delayed die swelling
- rod climbing (Weissenberg effect)
- memory effects, creep, yield stress, viscoelastic effects
- ketchup, toothpaste, pitch (tar), liquid armor (kevlar), dry granular flows, . . .

Non-Newtonian fluids

Newtonian (incompressible) fluid

such as water, is characterized by the consitutive relations

$$\mathbf{T} = -p\mathbf{I} + 2\mu\,\mathbf{D}, \qquad \operatorname{tr}\mathbf{D} = \operatorname{div}\mathbf{v} = 0,$$

- μ dynamic viscosity, $\mu > 0$
- p, $\mathbf{v}$ pressure, velocity
- $\mathbf{T}$, $\mathbf{I}$, $\mathbf{D}$ Cauchy stress tensor, Identity tensor, symmetric part of the velocity gradient

Shear-thinning / shear-thickening fluids

$$\mathbf{T} = -p\mathbf{I} + 2\mu(|\mathbf{D}|)\,\mathbf{D}, \qquad \operatorname{tr}\mathbf{D} = \operatorname{div}\mathbf{v} = 0,$$

- μ dynamic viscosity, $\mu = \mu(|\mathbf{D}|)$
  decreasing: shear-thinning

Shear-thinning fluids, power-law

Shear-thinning fluids, power-law

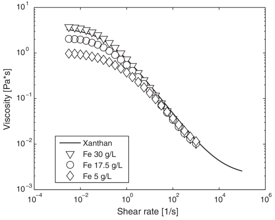

Fig. 3. Viscosity of NZVI-xanthan suspensions as a function of the shear rate. Since a replication was performed for every sample, the results were reported as the average of the two experiments.

From Comba, S.; Dalmazzo, D.; Santagaa, E.; Sethi, R. (2011, J. Hazard. Mater.)

Shear-thinning fluids, power-law

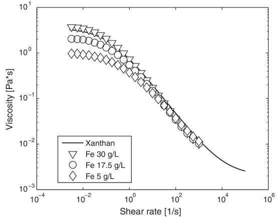

Fig. 3. Viscosity of NZVI-xanthan suspensions as a function of the shear rate. Since a replication was performed for every sample, the results were reported as the average of the two experiments.

From Comba, S.; Dalmazzo, D.; Santagaa, E.; Sethi, R. (2011, J. Hazard. Mater.)

Many different formulas

mainly developed by chemical engineers, e.g.

- Ostwald–de Waele *power-law* fluid

$$\mu = \mu_K |\mathbf{D}|^{n-1}, \qquad 0 < n < 1$$

Shear-thinning fluids, power-law

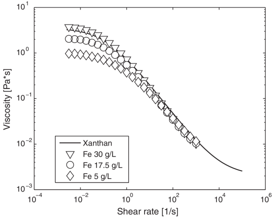

Fig. 3. Viscosity of NZVI-xanthan suspensions as a function of the shear rate. Since a replication was performed for every sample, the results were reported as the average of the two experiments.

From Comba, S.; Dalmazzo, D.; Santagaa, E.; Sethi, R. (2011, J. Hazard. Mater.)

Many different formulas

mainly developed by chemical engineers, e.g.

- Ostwald–de Waele *power-law* fluid

$$\boxed{\mu = \mu_K |\mathbf{D}|^{n-1}, \qquad 0 < n < 1}$$

- *Cross model*, or *Carreau–Yasuda model*

$$\mu = \mu_\infty + \frac{\mu_0 - \mu_\infty}{1 + \alpha |\mathbf{D}|^m}, \quad \text{or} \quad \mu = \mu_\infty + \frac{\mu_0 - \mu_\infty}{(1 + \alpha |\mathbf{D}|^2)^{m/2}}$$

Hagen–Poiseuille flow

Steady laminar simple flow in a (cylindrical) capillary:

for Newtonian fluid

$$Q_R = \frac{\pi R^4}{8\mu} \left| \frac{\partial P}{\partial x} \right| \qquad \Longrightarrow \qquad k_R = \frac{\phi_e}{8} R^2 .$$

Hagen–Poiseuille flow

Steady laminar simple flow in a (cylindrical) capillary:

for Newtonian fluid

$$Q_R = \frac{\pi R^4}{8\mu} \left| \frac{\partial P}{\partial x} \right| \qquad \Longrightarrow \qquad k_R = \frac{\phi_e}{8} R^2 .$$

for power-law fluid:

(remind: $\mu = \mu_K |\mathbf{D}|^{n-1}$, $0 < n < 1$)

$$Q_R = C_{(n,\eta_K)} R^{1+\frac{1}{n}} \left| \frac{\partial P}{\partial x} \right|^{\frac{1}{n}} \qquad \Longrightarrow \qquad k_R \equiv R^{1+\frac{1}{n}} .$$

Shear-thinning fluids

Increase the effectivity of remediation agents when treating the low permeability zones.

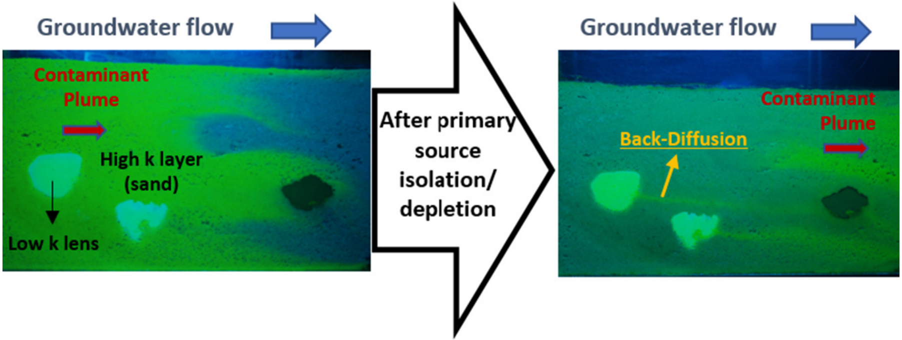

From F. Tatti et al. (2018) in Science of The Total Environment.

II. Capillary bundle model

Flux = Sum of fluxes.
. . . & non-Newtonian fluids.

Capillary bundle model

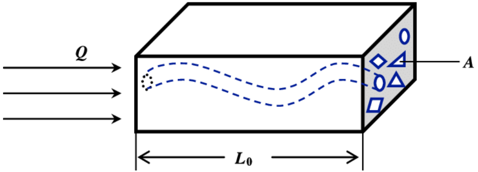

Make it better? Look inside?

Pore network modelling

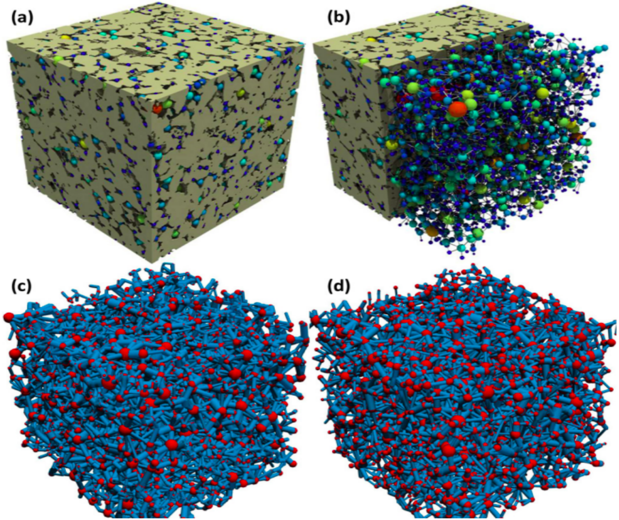

Make it better? Look inside?

Major issues in subsurface hydrology...

. . . are all related to

Make it better? Look inside?

Major issues in subsurface hydrology...

. . . are all related to

DATA.

Capillary bundle model

Effective pore size distribution

Capillary tubes of different pore sizes (for $\tau = 1$),

$$v \approx \sum_{i=1}^{N} w_i \, q(R_i), \qquad \text{with} \quad \sum_{i=1}^{N} w_i = \phi_e < 1,$$

or better

$$= \int_0^1 w(R)\, q(R)\, \mathrm{d}R \qquad \text{with} \quad \int_0^1 w(R)\, \mathrm{d}R = \phi_e < 1.$$

Capillary bundle model

Effective pore size distribution

Capillary tubes of different pore sizes (for $\tau = 1$),

$$v \approx \sum_{i=1}^{N} w_i \, q(R_i), \qquad \text{with} \quad \sum_{i=1}^{N} w_i = \phi_e < 1,$$

$$\text{or better} \quad = \int_0^1 w(R)\, q(R)\, \mathrm{d}R \qquad \text{with} \quad \int_0^1 w(R)\, \mathrm{d}R = \phi_e < 1.$$

Not so important for Newtonian fluids...

Note that (with $\tau = 1$):

$$k = \frac{\pi}{8} \sum_{i=1}^{N} w_i R_i^2 = \frac{\phi_e}{8} \frac{\sum_i w_i R_i^2}{\sum_i w_i} = \frac{\phi_e}{8} \bar{R}^2, \qquad \text{where} \quad \bar{R}^2 = \frac{\sum_i w_i R_i^2}{\sum_i w_i}.$$

Capillary bundle model for non-Newtonian fluids

Capillary bundle model

The total flux v sums the fluxes through capillaries of different size:

$$v(\nabla P, c) \approx \sum_{i=1}^{N} w_i\, q(\nabla P, c, R_i), \qquad \text{with} \quad \sum_{i=1}^{N} w_i = \phi_e < 1,$$

$$\text{or better} \quad = \int_0^1 w(R)\, q(\nabla P, c, R)\, \mathrm{d}R \qquad \text{with} \quad \int_0^1 w(R)\, \mathrm{d}R = \phi_e < 1,$$

where

- $v(\nabla P, c)$ . . . total volumetric (Darcy) flux
- ∇P . . . total pressure gradient (the forcing)
- c . . . parameter characterizing the fluid rheology, e.g. concentration of the aqueous solution of xanthan gum

Capillary bundle model for non-Newtonian fluids

Capillary bundle model

The total flux v sums the fluxes through capillaries of different size:

$$v(\nabla P, c) \approx \sum_{i=1}^{N} w_i \, q(\nabla P, c, R_i), \qquad \text{with} \quad \sum_{i=1}^{N} w_i = \phi_e < 1,$$

$$\text{or better} \qquad = \int_0^1 w(R) \, q(\nabla P, c, R) \, \mathrm{d}R \qquad \text{with} \quad \int_0^1 w(R) \, \mathrm{d}R = \phi_e < 1,$$

where

$v(\nabla P, c)$ . . . total volumetric (Darcy) flux
∇P . . . total pressure gradient (the forcing)
c . . . parameter characterizing the fluid rheology,
e.g. concentration of the aqueous solution of xanthan gum

and where

$R,\ R_i$ . . . effective pore sizes (pore radii), $\Longrightarrow$
$w(R),\ w_i$ . . . pore size weights (frequencies) $\Longrightarrow$ effective pore size distribution
$q(\nabla P, c, R)$ . . . volumetric flux (non-Newtonian Darcy law)
corresponding to pore size R.

III. Non-Newtonian porosimetry

Inverse problem.
Recent methods: YSM and ANA.

Inverse problem

The inverse problem of identifying the functional PSD

- Based on $v = v(\nabla P, c)$ measured experimentally...
- and assuming that, for given $q(\nabla P, c, R)$,

$$v(\nabla P, c) = \int_0^1 w(R)\, q(\nabla P, c, R)\, \mathrm{d}r$$

- we seek to find $w(R)$ based on the measured values of $v(\nabla P, c)$.

Inverse problem

Numerical porosimetry techniques

In the context of measuring the effective pore size distribution, this approach has been established in the yield stress fluid method (YSM) and the ANA method, see the references:

- Hauswirth S.C., Abou Najm M.R., Miller C.T. (2019) *Water Resour. Res. 55(8), 7182-7195*
- Abou Najm M.R., Atallah N.M. (2016) *Vadose Zone J. 15(9)*
- Rodriguez de Castro A., et al. (2020) *Comp. Chem. Eng. 133, 106662*

IV. Radial flow around an injected borehole

Far away: practical method.
Close enough: confined steady flow.
Numerical experiments.

(Work in progress.)

Radial flows

Far away goal

Check the possibility, whether the concept can be used for borehole testing in the future.

- There is no such *in-situ* measurement technique.
- Could be used for stratificated sediments?
- Could be used for borehole clogging tests?
- Let us start slowly, by small steps...

Radial flows

Nonlinear inverse problem

In the radial flow setting, the inverse problem is less straightforward and always nonlinear. The total flux of a shear-thinning fluid is distributed into the layers differently at each r.

We only have the data for ΔP, where

$$\Delta P(Q,c) = \int_{r_1}^{r_2} \nabla P\left(\tfrac{Q}{2\pi r}, c\right)\, \mathrm{d}r,$$

where $\nabla P(v,c)$ is itself a solution to the (nonlinear) equation:

$$v(\nabla P, c) = \sum_{i=1}^{N} v_i(\nabla P, c)\, w_i, \qquad \text{with} \quad \sum_{i=1}^{N} w_i = 1.$$

Radial flows

Numerical artificial data

Prior to designing the laboratory (or later, field) experiments, we study the numerical experiments based on artificial data.

We define a set of injection rates Q and a set of power-law fluids parametrized by c. The porous layers will have different characteristic pore sizes, providing us with distinct relations for $v_i(\nabla P, c)$. We chose a configuration of the layered media by prescribing the values of w_i.

For each Q and c, we compute the "observed" ΔP numerically.

Radial flows

Numerical algorithm: forward problem

- For given Q, c and $\{w_i\}_{i=1}^N$, the integral in (18) is discretized in r (log–equidistantly).
- At each r, the hydraulic gradient $\nabla P(\frac{Q}{2\pi r}, c)$ is computed numerically using the MATLAB `fzero` function.
- Additional random noise can be then added to ΔP.

Radial flows

Numerical algorithm: forward problem

- For given Q, c and $\{w_i\}_{i=1}^N$, the integral in (18) is discretized in r (log–equidistantly).
- At each r, the hydraulic gradient $\nabla P(\frac{Q}{2\pi r}, c)$ is computed numerically using the MATLAB `fzero` function.
- Additional random noise can be then added to ΔP.

Numerical algorithm: inverse problem

- Given a set of values of $\{Q_j\,,\ c_j\,,\ \Delta P_j\}_{j=1}^M$ (now ΔP simulated, instead of measured), we seek for $\{w_i\}_{i=1}^N$ by the nonlinear least squares fit of the forward problem, using the MATLAB `lsqnonlin` function.

Radial flows

Numerical results illustration

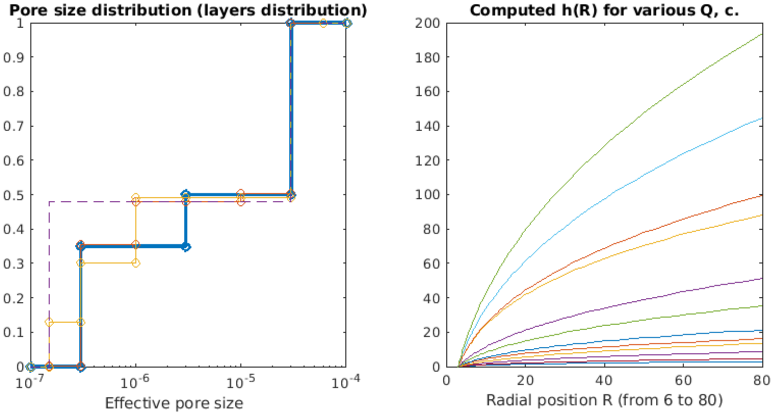

Left: the original distribution of layers (blue, thick) and its reconstructions: from the exact data (red), the data with 1% (yellow) or 2% (magenta, dashed) noise. Right: the hydraulic heads $h(r)$ of the artificial dataset.

Thank you for your attention!

Selected issues

Sensitivity, uniqueness & robustness

...

(work in progress)

Sensitivity of computed PSD to data error

For simplicity of presentation:

- Radii r_i given, we seek for the weights w_i.
- The algorithm is based on the one used in.[1] The least squares approximation with nonnegative weights is sought by Matlab `lsqlin` solver.
- The data are very nice (much nicer than real!):
  - artificial PSD $w(R)$ is given, with three Gaussian peaks;
  - the "measured" fluxes $v(\nabla P)$ corresponding to a set of hydraulic gradients ∇P are computed via the forward problem;
  - only one fluid is used, the rheology being described by Cross model, Hagen–Poiseuille flow (cylindrical capillary, no tortuosity) is computed numerically;
  - random relative 1% noise (normally distributed) is then added to the data.

[1] Abou Najm M.R., Atallah N.M. (2016). *Vadose Zone J.* 15, 1–5.

Sensitivity of computed PSD to data error

Example 1a: basic set of data

Here the hydraulic gradients generating the data correspond to the pore radii (similarly to YSM). 50 observations and 50 radii (full red:exact; circles: without noise; dashed: 1% noise).

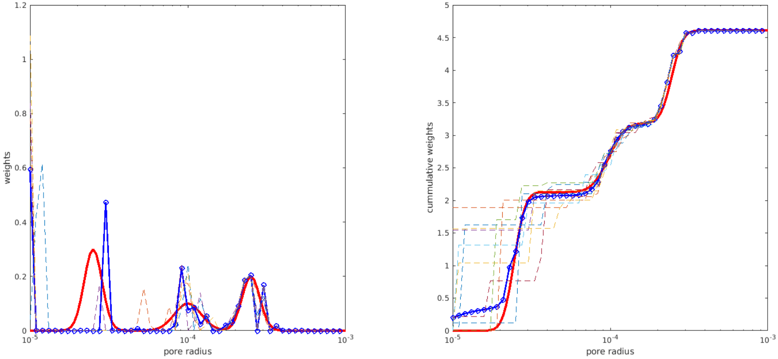

Note that the data error is only affecting the predicted radii of the small pores, but the error in cummulative weights remain low. Often, the peak is shifted to the lowest available pore size.

Errata: do not mind the vertical axis, the numbers are wrong. The LHS blue plot is also wrong.

Sensitivity of computed PSD to data error

Example 1b: basic set of data

Here the hydraulic gradients generating the data correspond to the pore radii (similarly to YSM).
12 observations and 12 radii (full red:exact; circles: without noise; dashed: 1% noise).

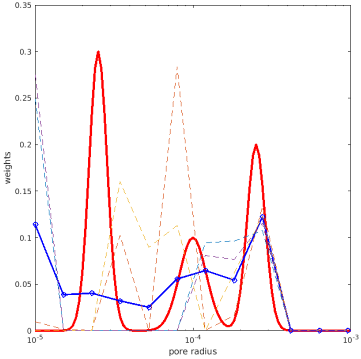

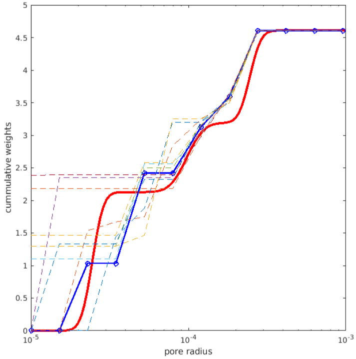

Similar to the previous larger problem. Again, the peak is often shifted to the left border.

Errata: do not mind the vertical axis, the numbers are wrong. The LHS blue plot is also wrong.

Sensitivity of computed PSD to data error

Example 2a: insufficient data

Here the higher hydraulic gradients are missing from the data set.
50 observations and 50 radii (full red:exact; circles: without noise; dashed: 1% noise).

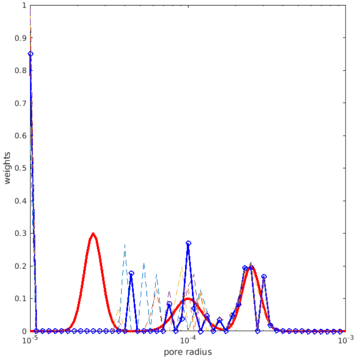

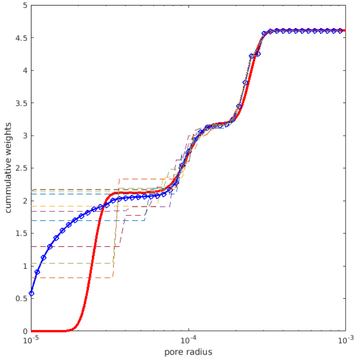

Note that the smaller pore sizes are badly resolved even with exact data, and with the noised data the error is spreading to the medium pore sizes.

Errata: do not mind the vertical axis, the numbers are wrong. The LHS blue plot is also wrong.

Sensitivity of computed PSD to data error

Example 2b: insufficient data

Here the higher hydraulic gradients are missing from the data set.
12 observations and 12 radii (full red:exact; circles: without noise; dashed: 1% noise).

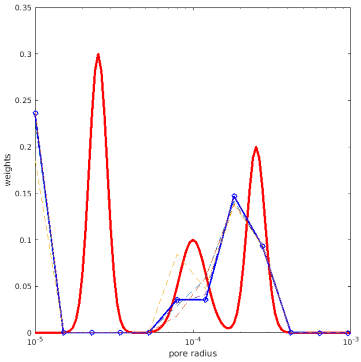

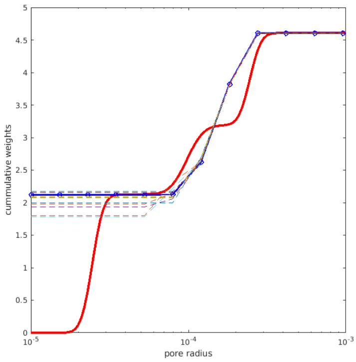

Here the left peak is shifted completely out of the border. The data set is cleary insufficient to capture the small pore sizes.

Errata: do not mind the vertical axis, the numbers are wrong. The LHS blue plot is also wrong.

Sensitivity of computed PSD to data error

Example 3a: insufficient data

Here the lower hydraulic gradients are missing from the data set.
50 observations and 50 radii (full red:exact; circles: without noise; dashed: 1% noise).

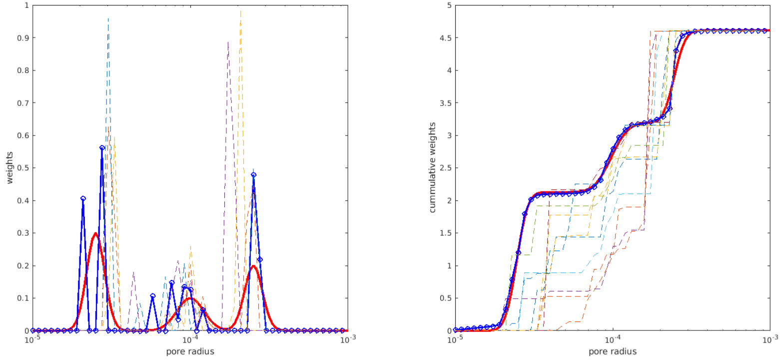

While the inversion for exact data seems perfect, the noice strongly affects the solution. Note the difference to the previous examples: here both peaks seem to be pulled to the middle.

Errata: do not mind the vertical axis, the numbers are wrong. The LHS blue plot is also wrong.

Sensitivity of computed PSD to data error

Example 3b: insufficient data

Here the lower hydraulic gradients are missing from the data set.
12 observations and 12 radii (full red:exact; circles: without noise; dashed: 1% noise).

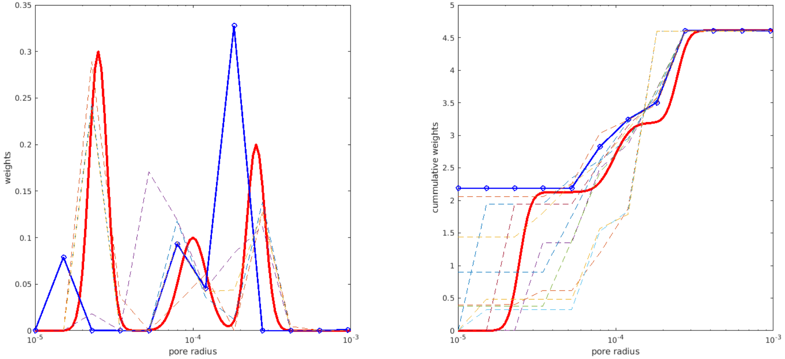

Similarly to the previous one, the inversion for exact data is not so bad except for the lowest peak shifted to the left border. Importantly, the inversion is quite sensitive to data noise.

Errata: do not mind the vertical axis, the numbers are wrong

Selected Issues

. . . anyone can invent *problems*, whether one has a computer or not. . .

General issues

- Given the experimental data,
  what is the optimal representative PSD and the best numerical algorithm to reach it?
- Given the data, the algorithm and the results,
  what is the reliability of the solution and the estimated error?
- Given a rough expectation about the pore size distribution,
  how to plan the optimal set of experiments (polymer concentrations, pressure drops)?

Selected Issues

. . . anyone can invent *problems*, whether one has a computer or not. . .

General issues

- Given the experimental data,
  what is the optimal representative PSD and the best numerical algorithm to reach it?
- Given the data, the algorithm and the results,
  what is the reliability of the solution and the estimated error?
- Given a rough expectation about the pore size distribution,
  how to plan the optimal set of experiments (polymer concentrations, pressure drops)?

Let us mention yet a few more:

- How to address these questions numerically, e.g. for $q(\dots, r)$ defined numerically for more realistic pore geometries and rheologies?
- How to measure/define, the quality/error of the computed representative PSD?
- How to measure the reliability of the method?

Selected issues

Two aspects of the same inverse problem

should be distinguished in attempts to better understand the methods.

- First, the performance of the discrete inversion:
  Given the data (exact or subject to random noise) that correspond to a pore size distribution with only a finite (small) N distinct pore sizes, how does different algorithms and different data sets perform in identifying this discrete pore size distribution?
- Second, the approximation of the PSD by the (discete) representative PSD:
  Given the pore size distribution that is continuous (or represented by a large number of pore sizes, e.g. the Gaussian peaks in the previous examples), what are its good approximations by small number of distinct pore sizes?

While mixed together in real applications, these aspects represent different mathematical issues.